Supporting Information

Nagamanasa et al. 10.1073/pnas.1101858108

SI Text

Histograms. To determine the temporal cut-off for identifying a colloid as a part of a grain boundary (GB), we have plotted the distributions of the fraction of time a particle is amorphous-like for all the GBs studied. The sampling region included the GB as well as the adjacent crystallites such that at any given instant in time, the number of amorphous-like particles is nearly equal to the number of crystal-like particles. Because particles within the bulk of the crystal remain crystal-like for most of the time, one would expect a peak in the distribution at small fractions. Also, one would expect particles in the GB to remain amorphous-like for most of the time and thus give rise to a peak at high fractions. In addition to these, there would be particles, at the interface, that fluctuate between crystal-like and amorphous-like states.

As shown in Fig. S1*A*, all GBs yielded a nearly bimodal distribution with a minimum value close to 50%, which we chose to be our temporal cut-off. Accordingly, particles which were amorphous-like for at least 50% of the duration of the experiment were identified as GB particles.

We have plotted the mean squared displacements (MSD) for $\Theta = 24.3°$ for different temporal cut-off values (Fig. S1*B*). We observed parallel shifts in the MSD profiles and only a 10% change in the intermediate time exponent, ν for a 40% change in the temporal cut-off value, ensuring that the cut-off procedure does not significantly alter our findings.

Low Angle Grain Boundaries. Low angle grain boundaries (LAGBs) consist of a periodic array of discrete dislocation cores (1). Fig. S2*B*, corresponding to a Θ of 10.4°, shows the dislocation cores obtained from a Voronoi tessellation of the image shown in Fig. S2*A*.

Radial Pair-Correlation Function. The local order of high misorientation angle grain boundaries (HAGBs) has been investigated using the radial pair-correlation function, $\langle g(\bar{r})\rangle$. Because of the complex shape of the grain boundary, an alternative procedure has been adopted to calculate $\langle g(\bar{r})\rangle$. First, to avoid the contribution coming from the surrounding crystalline regions to $\langle g(\bar{r})\rangle$, only particles belonging to the GB region are considered. We then temporally average the particle positions over a suitable time window, which in this case is 5 s, to eliminate the effects due to thermal motion and to preserve the underlying structure (2, 3). Using these average GB particle positions we obtain the unnormalized $\langle g(\bar{r})\rangle$. In the standard procedure, the normalization is the area of the annulus formed by concentric circles of radii r and $r + dr$. Because only GB particles are considered here, for r greater than the grain boundary width, such an annulus is not entirely contained in the GB region and therefore will underestimate the number of GB particles contributing to the annulus. To circumvent this problem, we have modified the normalization procedure as follows. For the radial pair-correlation function, the area under the first peak corresponds to the average number of nearest neighbors for a particle (4). We have determined this number by counting the number of nearest neighbors of each GB particle and averaging over all particles in the GB region and over all times. We rescale the unnormalized $\langle g(\bar{r})\rangle$ by a suitable multiplicative factor to ensure that the area under the first peak corresponds to the average number of nearest neighbors counted. Also, as the number of particles increases linearly with r, we obtain the normalized $\langle g(\bar{r})\rangle$ by further rescaling with $1/r$.

The resulting $\langle g(\bar{r})\rangle$ has been shown in Fig. S3. The split-second peak in $\langle g(\bar{r})\rangle$ has subpeaks at $\sqrt{3}\sigma$ and just below 2σ that coincide with the crystal peaks (dashed vertical lines) for an hcp lattice (5). Also, we have temporally averaged the particle positions over various time windows and we observe that a window of 5 s is sufficient to prevent the smearing of peaks, while capturing the trend in $\langle g(\bar{r})\rangle$ as a function of the misorientation angle.

Anisotropic Diffusion. We have plotted the MSDs of GB particles along directions parallel and perpendicular to the GB plane for all HAGBs studied. Geometric confinement would imply slower diffusion along the confinement direction, which in our case is perpendicular to the GB plane. Indeed, we observe that the diffusion of GB particles is anisotropic. For all HAGBs the intermediate time exponents, $\nu_{\|}$, for displacements parallel to the GB plane are higher than the exponents, $\nu_{\perp}$, displacements perpendicular to the GB plane as shown in Fig. S4. These results emphasize the influence of geometric confinement on GB dynamics.

van Hove Correlation Function. We have plotted the distinct part of the van Hove correlation function $G_d^m(r,t)$ (6) for the top 10% most mobile GB colloids at various times. For cooperatively rearranging particles, the probability that the position of a mobile particle at $t = 0$ is occupied by another nearby mobile particle at $t = t^*$ is high (7). This high probability of particle replacement is reflected in $G_d^m(r,t)$ for the most mobile particles as a peak at $r = 0$ when t is t^*. For all boundaries, as shown in Fig. S5, we see a maximum in $G_d^m(r,t)$ at $r = 0$ when $t = t^*$ with a simultaneous decrease in the peak at $r = \sigma$ as t approaches t^* suggesting cooperative rearrangements.

Cooperatively Rearranging Regions. We have performed the string analysis for three distance cut-off values $\delta = 0.6$, 1, and 1.4σ, where σ is the particle diameter. As expected, we find that for a given Θ the maximum string length, $n_{\max}$ and $\langle n\rangle$ increase with δ. As observed in the case of $\delta = 1\sigma$ (Fig. 3), $P(n)$ versus n remains exponential for $\delta = 0.6\sigma$ as well as for 1.4σ as shown in Fig. S6 *A* and *B*. In addition, the trend in $n_{\max}$ and $\langle n\rangle$ as a function of Θ remains unchanged for all three δs.

We have also performed string analysis of the top 10% most mobile particles based solely on the magnitude for comparison. Here, a mobile particle belongs to a cluster only if it has a neighboring mobile particle within a distance of 1.4σ, the first minimum of $g(r)$ of a liquid. Fig. S6*C* shows GB colloids organized into strings. We find that for all three Θs and temperatures studied $P(n)$ decreases exponentially with n (Fig. S6 *D* and *E*). Also, $n_{\max}$ and $\langle n\rangle$ systematically increase with Θ.

1. Read WT, Shockley W (1950) Dislocation models of crystal grain boundaries. *Phys Rev* 78:275–289.
2. Yonezawa F (2004) *Solid State Physics*, eds Ehrenreich H, Turnbull D (Academic, New York), p 225.
3. Kimura M, Yonezawa F (1983) *Topological Disorder in Condensed Matter*, eds Yonezawa F, Ninomiya T (Springer, Berlin), p 80.
4. Hern CS, Silbert LE, Liu AJ, Nagel SR (2003) Jamming at zero temperature and zero applied stress: The epitome of disorder. *Phys Rev E Stat Nonlinear Soft Matter Phys* 68:0113061–01130619.
5. Bernal JD (1964) The Bakerian lecture, 1962. The structure of liquids. *Proc R Soc London Ser A* 280:299–322.
6. Sanyal S, Sood AK (1996) Cooperative jumps and hop-back motion in supercooled liquids near the glass trasition in binary colloids. *Europhys Lett* 34:361–366.
7. Donati C, et al. (1998) String-like cooperative motion in a supercooled liquid. *Phys Rev Lett* 80:2338–2341.

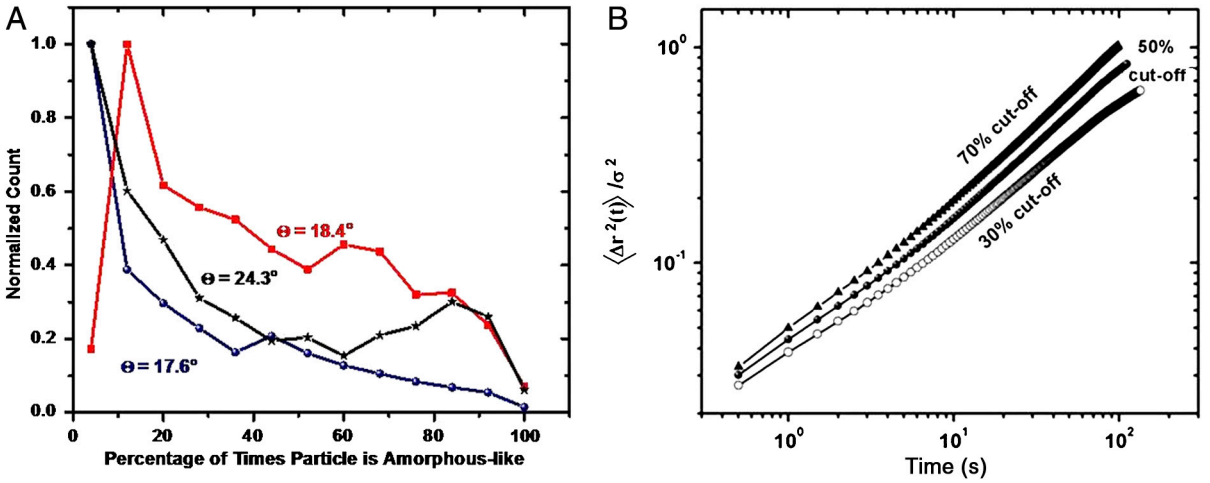

Fig. S1. (*A*) Frequency count of the fraction of time particles are amorphous-like for $\Theta = 24.3°$ (black stars), $\Theta = 18.4°$ (red squares), $\Theta = 17.6°$ (blue circles). The dashed lines correspond to a fourth-order polynomial fit to the data. (*B*) MSDs rescaled by σ^2, for $\Theta = 24.3°$ and $T = 299$ K for three different temporal cut-offs.

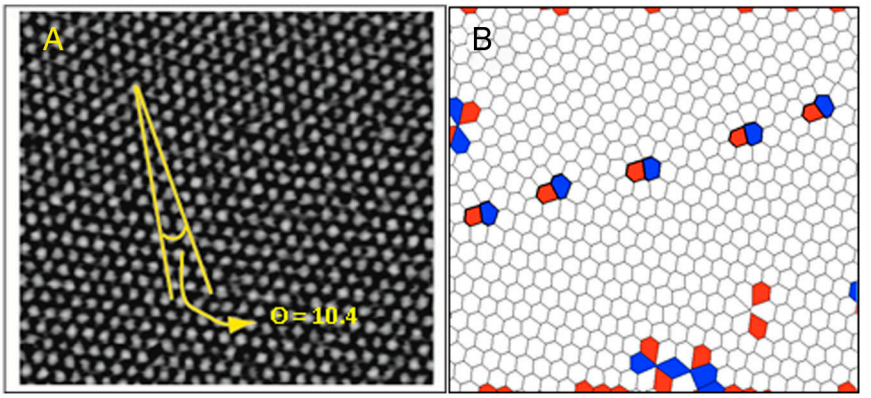

Fig. S2. (*A*) Image of LAGB. (*B*) Voronoi analysis of (*A*). The red and blue polygons along the GB correspond to the pentagon–heptagon pairs of the dislocation cores.

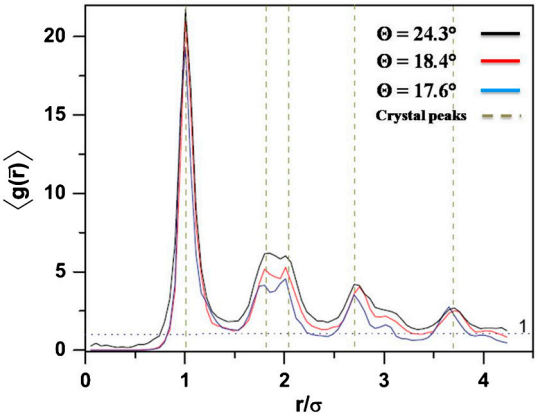

Fig. S3. Radial pair-correlation function $\langle g(\bar{r})\rangle$ for three Θs.

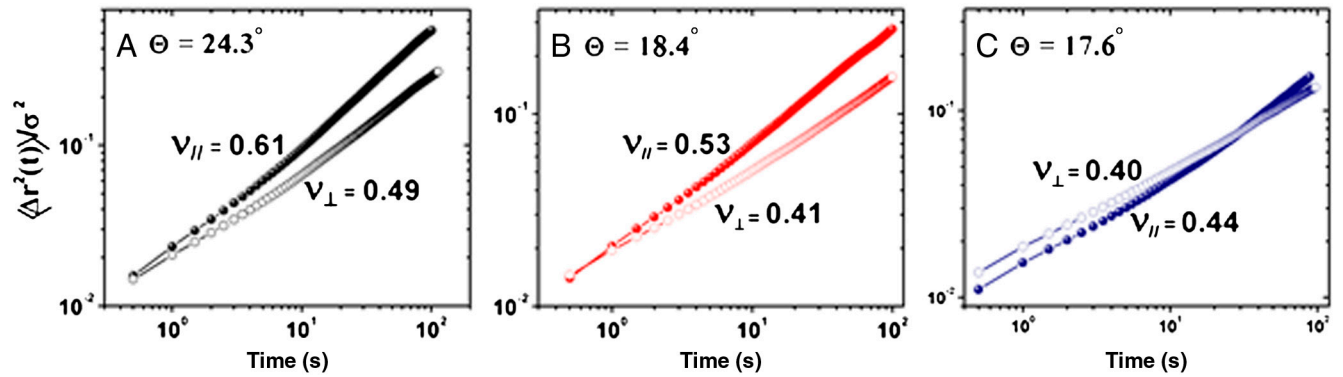

Fig. S4. Mean squared displacements (MSDs) rescaled by σ^2 for the direction parallel to the GB plane (solid symbols) and perpendicular to GB plane (hollow symbols). The symbols $\nu_{\|}$ and $\nu_{\perp}$ denote the exponents of MSDs parallel and perpendicular to the GB plane, respectively. (*A*) Mean squared displacements for $\Theta = 24.3°$ (black symbols), (*B*) $\Theta = 18.4°$ (red symbols), and (*C*) $\Theta = 17.6°$ (blue symbols).

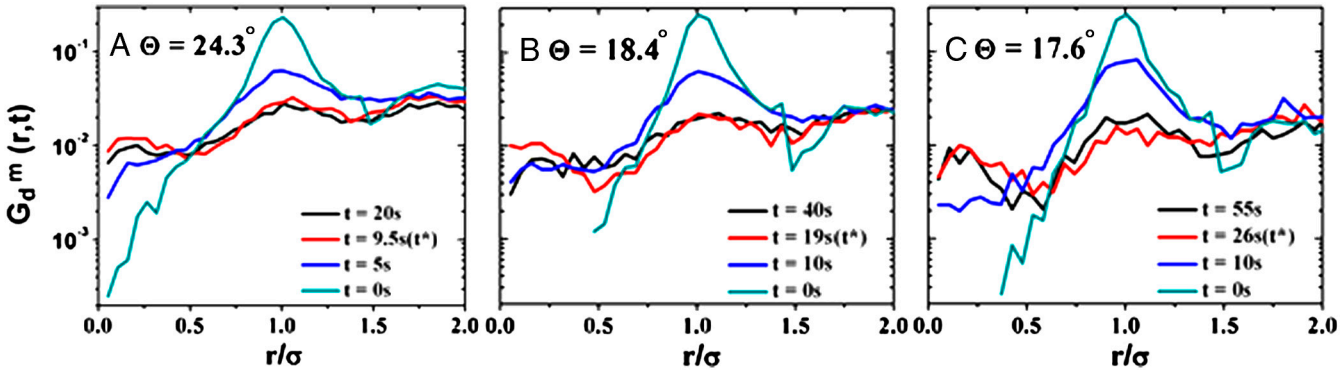

Fig. S5. The distinct part of the van Hove correlation function $G_d^m(r,t)$ as a function of r rescaled by σ, for mobile particles for three misorientation angles (*A*) $\Theta = 24.3°$, (*B*) $\Theta = 18.4°$, and (*C*) $\Theta = 17.6°$. The lines correspond to different Δt.

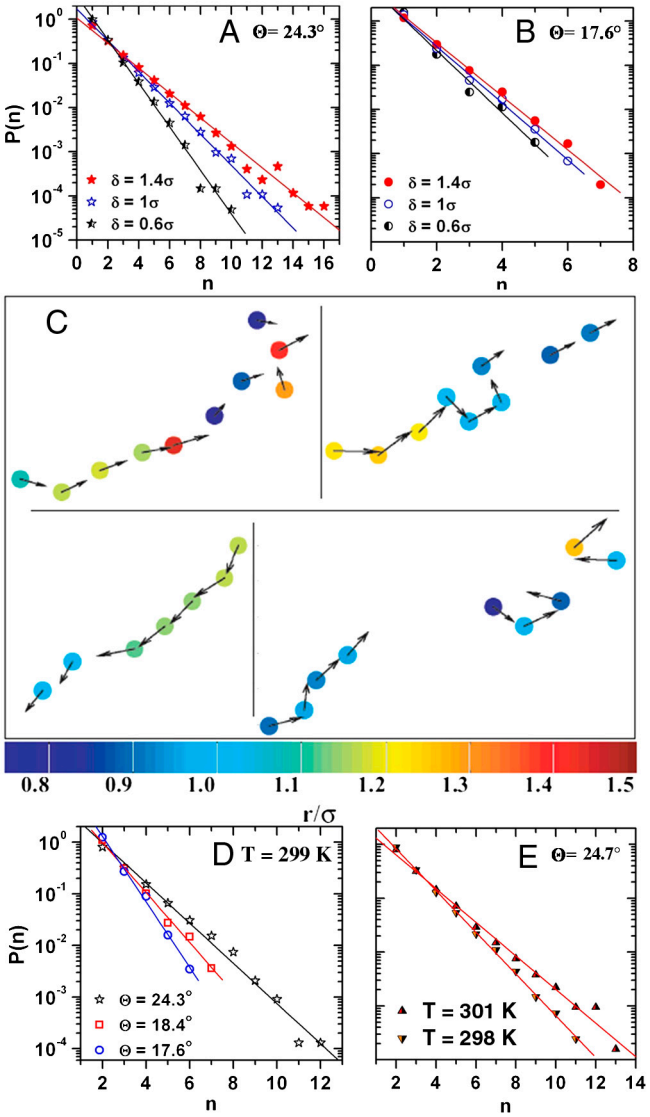

Fig. S6. Probability distribution of string lengths $P(n)$ versus n for different cut-offs δ for (*A*) $\Theta = 24.3°$ and (*B*) $\Theta = 17.6°$. (*C*) String-like motion of the most mobile particles taking into account only the magnitude of their displacements. The length of the arrow and the particle color code are according to the displacement magnitude. (*D*) $P(n)$ versus n for different Θs at $T = 299$ K. (*E*) $P(n)$ versus n for $\Theta = 24.7°$ at two temperatures.

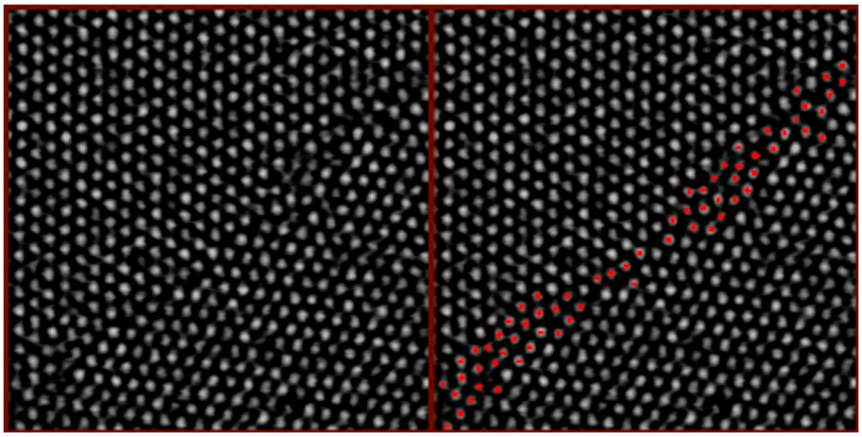

Movie S1 Dynamics of colloids at a GB for $\Theta = 24.3°$ and $T = 299$ K. Raw data (*Left*) and the GB colloids (*Right*, marked in red) identified using the method mentioned in the main text.

Movie S1 (MOV)

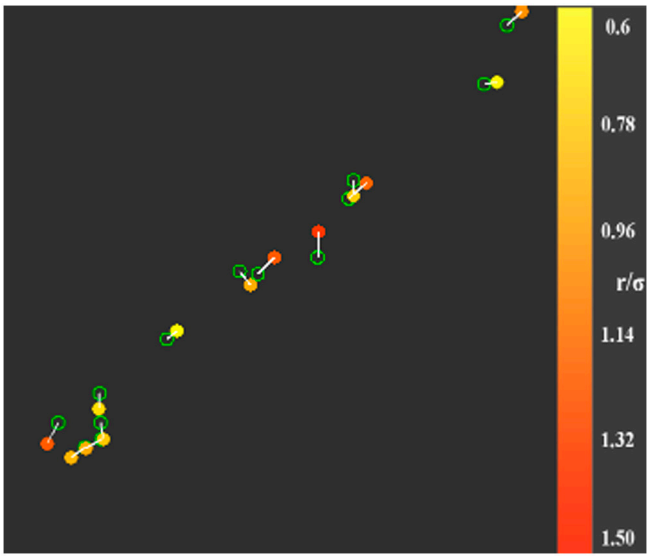

Movie S2 String-like cooperative rearrangements of the most mobile particles at a GB ($\Theta = 24.3°$ and $T = 299$ K). The particle positions at $t = 0$ are shown by the hollow green circles and their final positions at $t = t^*$ are shown by color-coded circles. The color code is according to the magnitude of their displacements.
Movie S2 (MOV)